

Supplementary Information

Expanding the design space of gel materials through ionic liquid mediated mechanical and structural tuneability

Alex P. S. Brogan^{1,2*}, Coby J. Clarke², Artemis Charalambidou², Colleen N. Loynachan³, Sarah E. Norman⁴, James Douth⁵, Jason P. Hallett².

1. Department of Chemistry, King's College London, Britannia House, London, SE1 1DB.

2. Department of Chemical Engineering, Imperial College London, London, SW7 2AZ, UK.

3. Department of Materials, Imperial College London, London, SW7 2AZ, UK.

4. ISIS Deuteration Facility, ISIS Neutron and Muon Source, STFC, Harwell Science and Innovation Campus, Didcot, Oxfordshire OX11 0QX, UK.

5. ISIS Neutron and Muon Source, STFC, Harwell Science and Innovation Campus, Didcot, Oxfordshire OX11 0QX, UK.

Materials and Methods

Ionogel fabrication

Photocrosslinked ionogels of polyethylene glycol diacrylate (PEGDA) were prepared at 5 – 40 wt% polymer with the following ionic liquids; 1-ethyl-3-methylimidazolium acetate ([emim][OAc]), 1-ethyl-3-methylimidazolium ethyl sulfate ([emim][EtSO₄]), 1-ethyl-3-methylimidazolium trifluoromethanesulfonate ([emim][OTf]), and 1-ethyl-3-methylimidazolium bis(trifluoromethylsulfonyl)imide ([emim][NTf₂]). In all cases, solutions of ionic liquid and polyethylene glycol diacrylate (M_n 575 g.mol⁻¹, 5 – 40 wt%) were prepared with 2 wt% 2-hydroxy-4'-(2-hydroxyethoxy)-2-methylpropiophenone as a photoinitiator. Solutions were then aliquoted into custom gel moulds and incubated at room temperature (21 ± 2 °C) and ambient humidity (40 – 50%) under constant irradiation at 365 nm (MLR-58 benchtop UV lamp) for 20 minutes to allow for crosslinking to go to completion. The resultant cylindrical ionogels of uniform diameters (12.5 mm, or 5 mm) were then stored in a desiccated environment until further use. Transparency of the resultant gels were dependent on the ionic liquid polarity, where the most polar ionic liquid ([emim][OAc]) gels were the least transparent, and the least polar ionic liquid ([emim][NTf₂]) gels were the most transparent. All chemicals were purchased from Sigma UK, and were used without further purification.

Deuterated ionic liquid synthesis

The deuterated ionic liquids followed the same procedures as the protiated analogues, but utilising deuterated precursor materials where appropriate.

Deuterated 1-ethyl-3-methylimidazolium acetate ([emim-d11][OAc-d3]), 1-ethyl-3-methylimidazolium trifluoromethanesulfonate ([emim-d11][OTf]), and 1-ethyl-3-methylimidazolium bis(trifluoromethylsulfonyl)imide ([emim-d11][NTf₂]) were all synthesized from a common source of deuterated methyl imidazole (hmim-d6). Here, hmim-d6 was prepared following the method of Hardacre *et al.*¹ and was then quaternised with bromoethane-d5 to prepare the [emim-d11][Br] intermediate. For [emim-d11][OAc-d3] and [emim-d11][OTf] species the bromide ionic liquid was converted to the hydroxide *via* treatment with Amberlite IRN-78 resin and then neutralised with the corresponding acid.² For [emim-d11][NTf₂], the bromide was treated with LiNTf₂ using established methods and conditions.³

For deuterated 1-ethyl-3-methylimidazolium methylsulfate [emim-d11][MeSO₄-d3], deuterated ethylimidazole-d8 was prepared following the procedure of Zhang *et al.*⁴ and subsequently treated with dimethylsulfate-d6 to yield the fully deuterated ionic liquid.⁵

Mechanical testing

Unconfined compressive stress-strain measurements were performed on cylindrical ionogels (12.5 x 7 mm) using an Instron 5543 (operated by Bluehill Universal Software) at room temperature and at a compression rate of 0.5 mm.min⁻¹. The compressive modulus of the gels at low and high strain were determined by the slope at the linear regions at low strain ($\leq 10\%$) and high strain (typically the region preceding failure) respectively for resultant plots of compressive stress against strain, and are reported as the average of triplicate measurements.

SANS measurements

Ionogels were prepared for SANS measurements as described above, using the deuterated ionic liquids as described above. Gels were cut to size using a scalpel and mounted in circular brass cells with a pathlength of 1 mm, 8 mm internal diameter, and quartz windows. SANS measurements were performed at 25 °C on the LOQ instrument at ISIS neutron and muon source with a neutron wavelength range of 2.2 – 10 Å, beam size of 6 mm, and SANS exposure of 40 μ A. Resultant 2D scattering plots were reduced to 1D profiles using ISIS in-house software and were fitted to a correlation length model using SASView.

XPS measurements

X-ray photoelectron spectra were recorded on a Thermo Fisher K-Alpha equipped with a 180° double focussing hemispherical analyser, 128-channel detector, and monochromated Al K α microfocused X-ray source ($h\nu = 1486.6$ eV) operated at 6 mA emission current and 12 kV anode bias. Slices of ionogel surfaces were mounted on a wellled copper plate and degassed to $<3 \times 10^7$ mbar before being transferred to the analysis chamber ($<2 \times 10^{-9}$ mbar). Each survey spectrum was recorded as five scans (5-6 minutes X-ray exposure) on a spot size of 400 μ m at 200 eV pass energy with a 0.5 eV step from -10 eV to 1350 eV. Samples were prevented from charging with a dual-beam flood source. Survey spectra can be found in the supporting information (SI Figure 1). Quantification was carried out in Avantage 5.951 using smart backgrounds and ALTHERMO1 RSFs; atomic compositions are tabulated in the supporting information (SI Table 2). Standard deviations were calculated from 5 different survey scans of each 30 wt% ionogel so that errors represent surface inhomogeneity, as well as preparation and measurement error. All ionogels analysed in this work were found to have excellent X-ray beam stability and were effectively charged neutralised due to the conductive ionic liquid components.

Supplementary Table 1. Hydrogen bond basicity for anions used in this study.

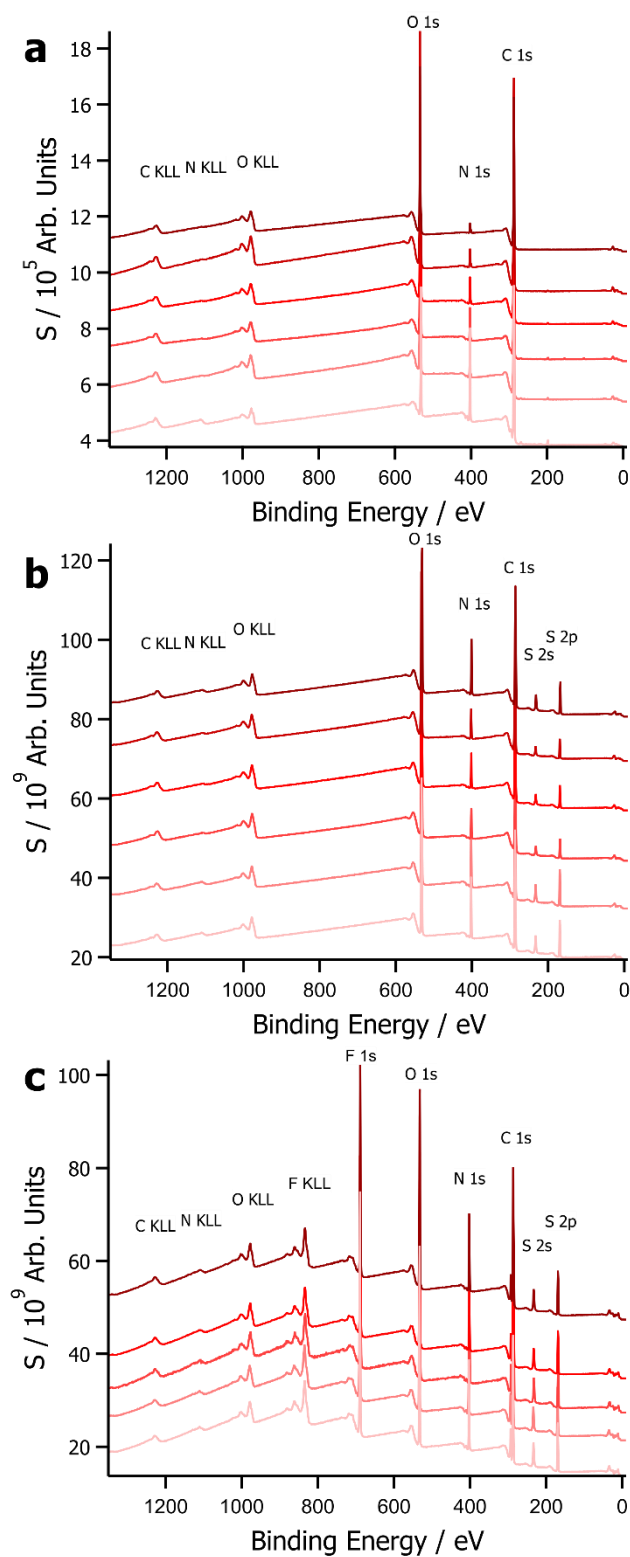
Anion	Formula	β	Reference
[OAc] ⁻	CH ₃ CO ₂ ⁻	0.85	6
[EtSO ₄] ⁻	C ₂ H ₅ SO ₄ ⁻	0.62	7
[OTf] ⁻	CF ₃ SO ₃ ⁻	0.48	6
[NTf ₂] ⁻	N(CF ₃ SO ₂) ₂ ⁻	0.23	6

Supplementary Table 2. Compressive modulus, failure stress, and failure strain for crosslinked PEGDA ionogels.

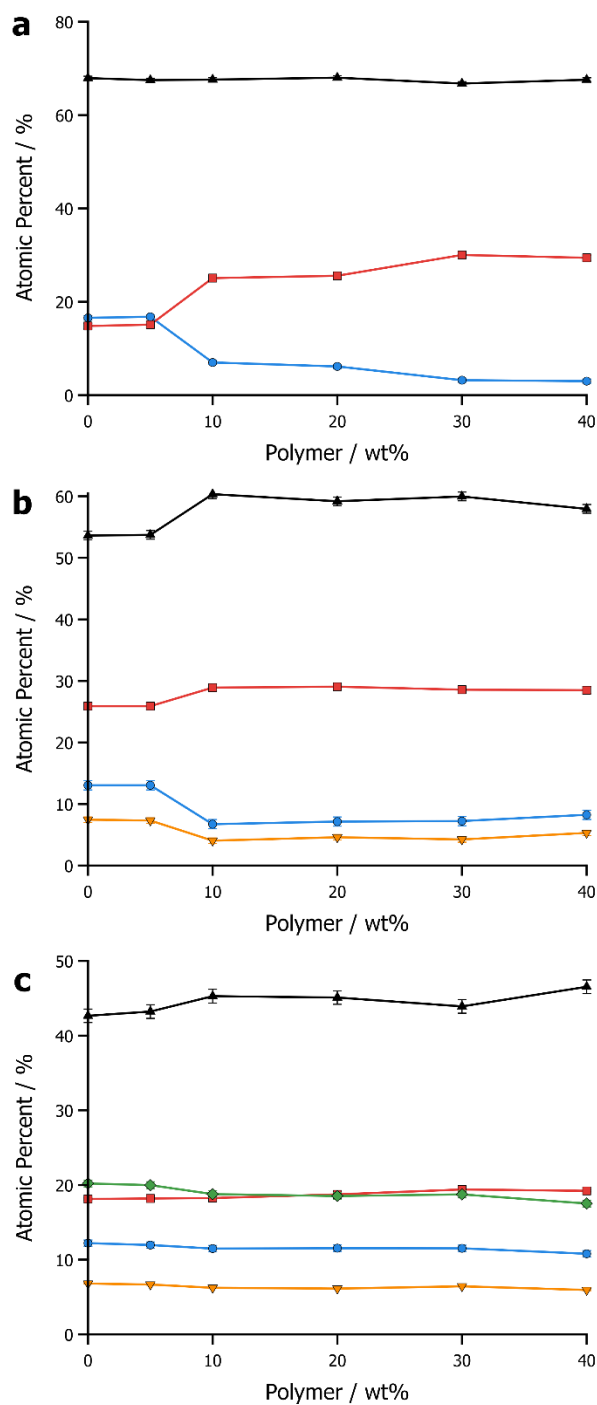
Ionogel		Compressive Modulus (Low strain) / MPa	Compressive Modulus (High strain) / MPa	Failure stress / MPa	Failure strain / %
[emim][OAc]	10 wt%	0.0014 ± 0.0010	0.26 ± 0.14	-	-
	20 wt%	0.0057 ± 0.0018	0.59 ± 0.24	0.08 ± 0.03	62.9 ± 4.0
	30 wt%	0.030 ± 0.012	0.84 ± 0.20	0.27 ± 0.09	64.8 ± 3.1
	40 wt%	0.058 ± 0.027	1.18 ± 0.34	0.54 ± 0.31	66.3 ± 13.9
[emim][EtSO ₄]	10 wt%	0.00069 ± 0.00033	0.77 ± 0.36	0.06 ± 0.01	56.2 ± 2.4
	20 wt%	0.0063 ± 0.0023	0.79 ± 0.12	0.14 ± 0.04	85.6 ± 9.5
	30 wt%	0.023 ± 0.0039	1.13 ± 0.12	0.26 ± 0.03	70.3 ± 5.9
	40 wt%	0.042 ± 0.014	4.16 ± 1.96	1.11 ± 0.38	75.8 ± 5.4
[emim][OTf]	10 wt%	0.029 ± 0.012	0.76 ± 0.10	0.10 ± 0.02	47.5 ± 2.6
	20 wt%	0.074 ± 0.0032	1.36 ± 0.49	0.26 ± 0.12	45.8 ± 8.1
	30 wt%	0.23 ± 0.075	8.23 ± 0.89	1.58 ± 0.16	54.0 ± 9.5
	40 wt%	0.27 ± 0.049	9.66 ± 2.43	1.87 ± 0.98	48.2 ± 2.5
[emim][NTf ₂]	10 wt%	0.022 ± 0.010	0.75 ± 0.26	0.12 ± 0.04	52.9 ± 1.6
	20 wt%	0.087 ± 0.026	3.37 ± 0.54	0.61 ± 0.08	44.3 ± 2.9
	30 wt%	0.45 ± 0.10	10.13 ± 3.68	1.58 ± 0.60	43.0 ± 3.9
	40 wt%	0.57 ± 0.30	8.29 ± 3.52	0.90 ± 0.57	27.2 ± 4.6

Supplementary Table 3. Correlation length (ξ) and porod exponent (n) for ionogels as calculated to correlation length fits to SANS profiles (Fig. 4).

Ionogel		$\xi / \text{Å}$	n
[emim][OAc]	5 wt%	175.8	4.03
	10 wt%	47.6	4.47
	20 wt%	12.8	4.09
	30 wt%	12.2	3.91
	40 wt%	5.6	4.34
[emim][EtSO ₄]	5 wt%	92.4	5.27
	10 wt%	57.9	5.32
	20 wt%	25.4	4.71
	30 wt%	16.8	4.59
	40 wt%	16.4	4.43
[emim][OTf]	5 wt%	142.5	2.06
	10 wt%	209.4	1.72
	20 wt%	187.2	2.30
	30 wt%	180.3	2.00
	40 wt%	139.3	3.00
[emim][NTf ₂]	5 wt%	94.9	1.47
	10 wt%	130.2	2.76
	20 wt%	142.3	1.81
	30 wt%	175.0	1.58
	40 wt%	138.2	1.93



Supplementary Figure 1. XPS survey scans of ionogel surfaces with crosslinked PEGDA concentrations of 0, 5, 10, 20, 30, 40 wt% (light red – dark red) in [emim][OAc] (a), [emim][EtSO₄] (b), and [emim][OTf] (c).

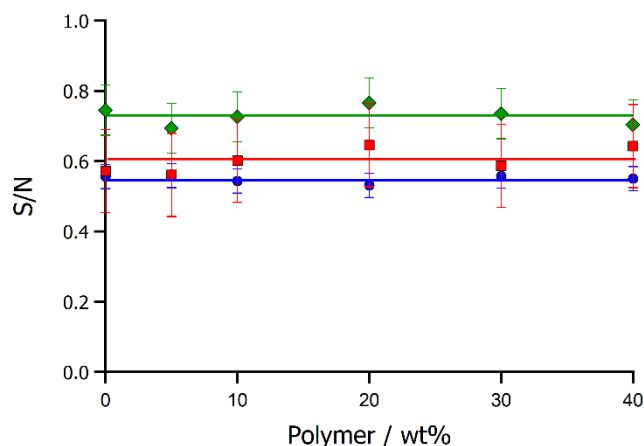


Supplementary Figure 2. Plots of atomic percent (calculated from XPS survey scans – SI Fig. 1) against PEGDA content for ionogels with [emim][OAc] (a), [emim][EtSO₄] (b), and [emim][OTf] (c). Plots show carbon (black triangles), oxygen (red squares), nitrogen (blue circles), fluorine (green diamonds), and sulfur (yellow upside down triangles).

Supplementary Table 4. Atomic composition (%) of ionic liquids and ionogels as determined by XPS survey scans (SI Fig. 1).

IL	PEG	Composition (%)							
		C	N	O	F	Si	S	Cl	
	RSF^a	1.00	1.68	2.89	0.90		1.89	2.74	N/O
[emim][OAc]	40	67.57	3.01	29.42					0.10
	30	66.75	3.21	30.04					0.11
	20	68.02	6.15	25.59				0.24	0.24
	10	67.60	6.99	25.07				0.34	0.28
	5	67.48	16.79	15.10				0.63	1.11
	0	67.94	16.58	14.81				0.67	1.12
	Initiator	68.41	16.14	14.81				0.64	1.09
	Theoretical	66.67	16.67	16.67					1.00
[emim][EtSO ₄]	40	57.94	8.26	28.49			5.31		0.29
	30	59.96	7.23	28.57			4.24		0.25
	20	59.19	7.14	29.06			4.61		0.25
	10	60.34	6.72	28.90			4.04		0.23
	5	53.72	13.05	25.91			7.32		0.50
	0	53.61	13.04	25.89			7.46		0.50
	Theoretical	53.33	13.33	26.67			6.67		0.50
[emim][OTf]	40	46.53	10.80	19.21	17.52		5.94		0.56
	30	43.92	11.53	19.39	18.74		6.43		0.59
	20	45.10	11.53	18.73	18.52		6.12		0.62
	10	45.27	11.48	18.24	18.77		6.24		0.63
	5	43.21	11.95	18.19	19.97		6.68		0.66
	0	42.66	12.22	18.12	20.20		6.80		0.67
	Theoretical	43.75	12.50	18.75	18.75		6.25		0.67
[emim][NTf ₂]	40	38.63	10.66	18.87	24.34		7.50		0.56
	30	35.98	11.64	17.80	26.02		8.56		0.65
	20	34.18	11.88	16.49	28.35		9.10		0.72
	10	33.37	12.56	16.63	28.32		9.12		0.76
	5	33.84	12.69	16.53	28.14		8.80		0.77
	0	33.62	12.57	16.23	28.21		9.37		0.77
	Theoretical	34.78	13.04	17.39	26.09		8.70		0.75

^aALThermo1



Supplementary Figure 3. Plot of the ratio of S to N (as calculated from atomic % data derived from XPS scans – SI Fig. 1, SI Table 4) against polymer content for [emim][EtSO₄] (red squares), [emim][OTf] (blue circles), and [emim][NTf₂] (green diamonds) ionogels.

References

- 1 C. Hardacre, J. D. Holbrey and S. E. J. McMath, *Chem. Commun.*, 2001, **1**, 367–368.
- 2 J. L. Ferguson, J. D. Holbrey, S. Ng, N. V. Plechkova, K. R. Seddon, A. A. Tomaszowska and D. F. Wassell, *Pure Appl. Chem.*, 2012, **84**, 723–744.
- 3 J. A. McCune, P. He, M. Petkovic, F. Coleman, J. Estager, J. D. Holbrey, K. R. Seddon and M. Swadźba-Kwaśny, *Phys. Chem. Chem. Phys.*, 2014, **16**, 23233–23243.
- 4 Y. Zhang, W. Zhu, Y.-L. Liu, H. Wang, K. Wang, K. Li, J. H. No, L. Ayong, A. Gulati, R. Pang, L. Freitas-Junior, C. T. Morita and E. Oldfield, *ACS Med. Chem. Lett.*, 2013, **4**, 423–427.
- 5 J. D. Holbrey, W. M. Reichert, R. P. Swatloski, G. A. Broker, W. R. Pitner, K. R. Seddon and R. D. Rogers, *Green Chem.*, 2002, **4**, 407–413.
- 6 A. F. M. Cláudio, L. Swift, J. P. Hallett, T. Welton, J. A. P. Coutinho and M. G. Freire, *Phys. Chem. Chem. Phys.*, 2014, **16**, 6593–601.
- 7 A. Jeličić, F. Köhler, A. Winter and S. Beuermann, *J. Polym. Sci., Part A Polym. Chem.*, 2010, **48**, 3188–3199.